Polarization-Dependent X-ray Absorption Spectroscopic Study of [Cu(cyclam)]$^{2+}$-Intercalated Saponite

Jin-Ho Choy,* Joo-Byoung Yoon, and Hyun Jung

National Nanohybrid Materials Laboratory, School of Chemistry and Molecular Engineering, Seoul National University, Seoul 151-747, Korea

Received: February 7, 2002; In Final Form: July 16, 2002

The [Cu(cyclam)]$^{2+}$ (copper-1,4,8,11-tetraazacyclotetradecane)−saponite complex has been obtained by an ion exchange reaction, and a thin film for the [Cu(cyclam)]$^{2+}$−saponite complex has been prepared by spin-coating onto glass slides. The orientation and the structural change of the guest complex ion in the interlayer space of saponite have been investigated using X-ray diffraction (XRD) and polarization-dependent X-ray absorption spectroscopy (XAS). The interlayer thickness of 3.75 Å from XRD analysis suggests that the copper complex ions are intercalated as a monolayer with the square planes of (Cu−N_4) parallel to the silicate layers. Angle-resolved Cu K-edge XAS from 10 to 80° for the incident beam shows the well-resolved peak intensity variation of the *xy* (in-plane) and *z* (out-of-plane) components. From the polarized Cu K-edge X-ray near-edge spectroscopic (XANES) analysis, all the peaks can be assigned to the in-plane and out-of-plane components. The change of the bonding character also can be explained by the amount of LMCT (ligand-to-metal charge transfer). The Cu−N bonds in the [Cu(cyclam)]$^{2+}$ complex within the interlayer space of saponite show more covalent character compared to those of [Cu(cyclam)]$(ClO_4)_2$ but less covalent character compared to those of [Cu(cyclam)]−montmorillonite and [Cu(cyclam)]−hectorite, which is attributed to the amount of LMCT due to the difference in the magnitude of the layer charge of these clays as well as the difference in the origin of the layer charge of the silicate.

Introduction

Recently, great interest has been expressed in the intercalation chemistry of two-dimensional (2-D) compounds because of their potential application as catalysts, sorbents, molecular sieves, secondary batteries, and electrochromic displays.[1] Among such 2-D compounds, natural or synthetic clays in particular have attracted a great deal of attention because they can accommodate various cationic species, regardless of whether they are inorganic or organic ions or even polymeric ions, within their interlayer space. Therefore, extensive studies have paid attention to the intercalation chemistry of these layered aluminosilicates.[2,3]

For example, ions and molecules including metal−organics intercalated into the layered aluminosilicates can be altered in their electronic structure via interaction with the negatively charged layers, which may provide improved stability and enhanced reactivity in catalytic reactions.[2−4] Therefore, the elucidation of the chemical bonding state as well as the local structure of transition-metal ions within the layers has been one of the most attractive problems in intercalation chemistry.

However, the intercalation complexes obtained by soft chemistry are often poor in crystallinity because they suffer from considerable elastic deformation during the intercalation reaction. Therefore, the conventional diffraction technique is not appropriate for resolving their crystal structures, especially for probing the local environment around the metal ion in guest molecules intercalated in aluminosilicate. Alternative methods such as diffuse reflectance UV−visible absorption and X-ray photoelectron (XPS) spectroscopy usually offer only an indirect probe of the metal ion. In this regard, the X-ray absorption spectroscopic (XAS) method, combined with X-ray diffraction (XRD), is thought to be useful not only for resolving the crystal structures of such complex materials[5] but also for investigating the local symmetry, electronic structure, and oxidation state of specific elements in the lattice.[6,7]

We have previously studied the intercalation of the [Cu(cyclam)]$^{2+}$ (copper-1,4,8,11-tetraazacyclotetradecane) complex ion, which exhibits significant catalytic activity in many reactions including important electrochemical, biological, and photobiological processes,[8,9] into negatively charged natural clays such as montmorillonite and hectorite.[10,11] We could successfully probe the relationship between the covalent (Cu−N) bond and the catalytic activity by the Cu K-edge XAS technique. However, as previously indicated, the spectra for the nonoriented powder samples reflect a superposition of all edge transitions in both the bound state and the continuum regimes, so an interpretation of the X-ray absorption near-edge structure (XANES) region is generally quite complicated. As a result, there has been a lot of ambiguity and much contention in the peak assignments of XANES spectra of transition-metal compounds.[10]

In the present study, we have applied a classical polarization XAS technique to the layered intercalation complex system and have tried to demonstrate how its intrinsic structural low-dimensionality could be utilized in the XANES peak assignments. In addition, the usefulness and constraints in the application of the XAS method to the 2-D material are discussed. Finally, we investigated the evolution of the bonding character and the local structure of the [Cu(cyclam)]$^{2+}$ ion in saponite by comparing them in montmorillonite and hectorite complexes[10,11] as well as in [Cu(cyclam)]$(ClO_4)_2$ aqueous solution itself.

* Corresponding author. E-mail: jhchoy@plaza.snu.ac.kr. Tel: +82-2-880-6658. Fax: +82-2-872-9864.

10.1021/jp020374+ CCC: $22.00
Published on Web 10/08/2002

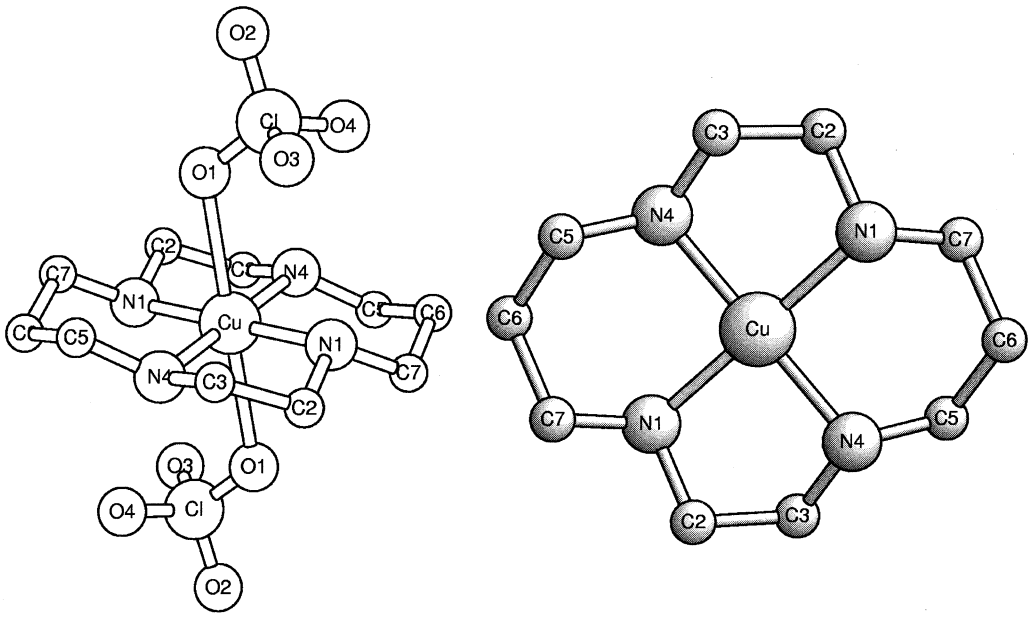

Figure 1. Schematic description of [Cu(cyclam)]$(ClO_4)_2$ (left) and top view of [Cu(cyclam)]$^{2+}$ ion (right).

Experimental Section

Sample Preparation. Synthetic saponite supplied from Kunimine Ind. Co. (Smecton SA) was used for an ion-exchange reaction. Its chemical formula and CEC were determined to be $Na_{0.36}(Mg_{2.99}Al_{0.01})(Si_{3.63}Al_{0.37})O_{10}(OH)_2$ and 80 meq/100 g, respectively. The elemental composition of this clay showed that 97% of isomorphous substitution took place in the tetrahedral sheets.[12]

[Cu(cyclam)]$(ClO_4)_2$ was prepared as previously reported.[10] For the formation of [Cu(cyclam)]$^{2+}$−saponite intercalate, saponite (1.0 g) was immersed in [Cu(cyclam)]$^{2+}$ aqueous solution (∼1.0 g/10 mL) at 60 °C for a week. The exchanged clay was centrifuged and washed several times with deionized water to remove the excess salt. The wet [Cu(cyclam)]$^{2+}$−saponite complex thus obtained was dispersed in distilled water and then spin coated onto a slide glass. Finally, the film and the wet powder were freeze dried in a vacuum ($<10^{-5}$ Torr).

Characterization. X-ray diffraction patterns for the powder intercalate and the film were recorded by a Philips diffractometer system (PW1830) using Ni-filtered Cu Kα radiation (λ = 1.54184 Å) operated at 40 kV and 20 mA.

X-ray absorption measurements were carried out with synchrotron radiation by using the EXAFS facilities installed at beam lines 7C and 10B of the Photon Factory (KEK, Tsukuba), operated at 2.5 GeV with ca. 350−400 mA of stored current. The polarization-dependent XAS for the film was taken at the Cu K-edge with a fluorescence mode by using a Lytle-type detector at beam line 7C. A Si(111) double-crystal monochromator was used. The XAS data for [Cu(cyclam)]$^{2+}$−saponite and a [Cu(cyclam)]$(ClO_4)_2$ powder sample and its aqueous solution were recorded in transmission mode at beam line 10B by using the ionization chambers filled with N_2 (25%) + Ar (75%) and N_2 (100%) for incident and transmitted beams, respectively, at room temperature. A Si(311) channel-cut monochromator was employed. To ensure the reliability of the spectra, much care has been taken to evaluate the stability of the energy scale by monitoring the spectrum of copper metal (E_0 = 8979 eV) for each measurement, and thus the edge positions were reproducible to better than 0.05 eV.

XANES and EXAFS Data Analysis. The data analyses for the experimental spectra were performed by the standard procedure, as previously described.[13−15] Photon energies of all XANES spectra were calibrated from the first absorption peak of the copper metal foil spectrum, defined to be at 8979 eV. The inherent background in the data was removed by fitting a polynomial to the preedge region and extrapolating through the entire spectrum, from which it was subtracted. The absorbance $\mu(E)$ was normalized to an edge jump of unity to compare the XANES features directly with one another. EXAFS curve fitting was carried out by using the UWXAFS2.0 code[16] on the basis of the following EXAFS equation:

$$\chi(k) = -S_0^2 \Sigma_i N_i F_i(k) \exp(-2\sigma_i^2 k^2) \exp\{-2R_i/\lambda(k)\} \sin\{2kR_i + \phi_i(k)\}/(kR_i^2)$$

The backscattering amplitude, $F_i(k)$, the total phase shift, $\phi_i(k)$, and the photoelectron mean free path, $\lambda(k)$, have been theoretically calculated for all scattering paths including multiple scatterings by the curved-wave ab initio EXAFS code FEFF 6.[17,18] In the course of nonlinear least-squares curve fitting between the experimental EXAFS spectrum and the theoretical spectrum, the coordination number, N_i, was fixed to the crystallographic value, and the other structural parameters such as bond distance, R_i, the Debye−Waller factor, σ_i^2, and the threshold energy difference, ΔE_0, were optimized as variables.

Results and Discussion

Structural Aspects of [Cu(cyclam)]$(ClO_4)_2$ and Saponite. The crystal system of [Cu(cyclam)]$(ClO_4)_2$ is triclinic with space group $P\bar{1}$.[19] The coordination sphere of the copper ion is defined by a planar arrangement of the four nitrogen atoms in the macrocyclic ligand, with oxygen atoms from the perchlorate groups lying above and below this plane, as shown in Figure 1. The resulting tetragonally distorted octahedron of donor atoms gives the interatomic distances of the (Cu−N) bond as 2.017 and 2.023 Å and the distance of the (Cu−O) bond as 2.567 Å.

Saponite belongs to the group of expanding layer-lattice silicate minerals known as smectites.[20] Each layer is composed of a sheet of octahedrally bonded cations sandwiched between two sheets of SiO_4 tetrahedra, as shown in Figure 2. Saponite has a unit-cell structure that consists of 20 oxygen atoms and 4

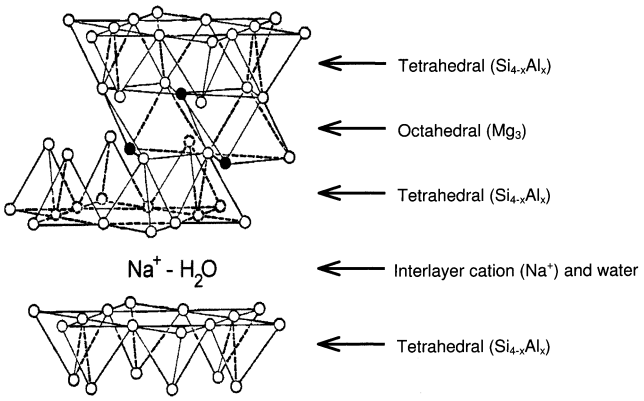

Figure 2. Schematic description of sodium saponite: (●), $(OH)^-$; (○), oxygen.

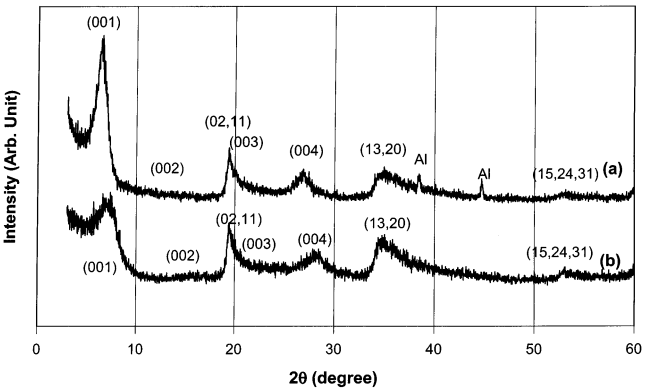

Figure 3. Powder X-ray diffraction patterns for saponite (b) and its $[Cu(cyclam)]^{2+}$ intercalation complex (a).

OH groups. These 2:1-type layers are continuous in the $\vec{a}$ and $\vec{b}$ directions and are stacked one above the other in the $\vec{c}$ direction. The isomorphous substitution of the Al^{3+} for the Si^{4+} ion in the tetrahedral layer results in the formation of fixed negative charges that are balanced by interlayer cations in the interlayer space. Usually, it is characterized by a layer charge of ca. 12 per unit cell. This interlayer space is also normally occupied by solvated water or organic polar molecules. The $\vec{c}$ axis spacing is, therefore, not fixed but varies depending on the nature of the exchanged cations, the degree of solvation, and the size and geometry of the organic molecules. If the exchanged cation is a transition-metal ion, the complex in the interlayer could be easily formed by reacting with electron-donating ligands.[21] The coordination chemistry of the metal ion is often similar to that of the ion in solution but frequently is strongly influenced by the charged silicate surface.[10]

Powder X-ray Diffraction Analyses. The intercalation of the $[Cu(cyclam)]^{2+}$ ion into saponite was confirmed by powder XRD, as shown in Figure 3. The (001) and (004) peaks of $[Cu(cyclam)]^{2+}$ intercalated saponite shifted to lower angles than those of Na−saponite because of the dimensions of the bulky copper organo complex. The (001) and (004) diffraction peaks at $2\theta = 6.49$ and 26.80° give a basal spacing of $d = 13.35$ (±0.05) Å. The thickness of the intercalated layer, estimated to be 3.75 Å by subtracting the 9.60 Å layer thickness of saponite from the observed d spacing, suggests that the copper complex ions are intercalated as a monolayer with the square planes of (Cu−N_4) parallel to the silicate layers and that the axial oxygen ligands from the ClO_4^- group have been replaced by silicate lattices. Despite the expansion of the $\vec{c}$ axis, the $\vec{a}$ and $\vec{b}$ axis parameters of 5.44 and 9.19 Å, estimated from the (06, 13) and (02,11) peaks, were nearly invariant after the intercalation, implying that the ion-exchange reaction proceeds topotactically.[20]

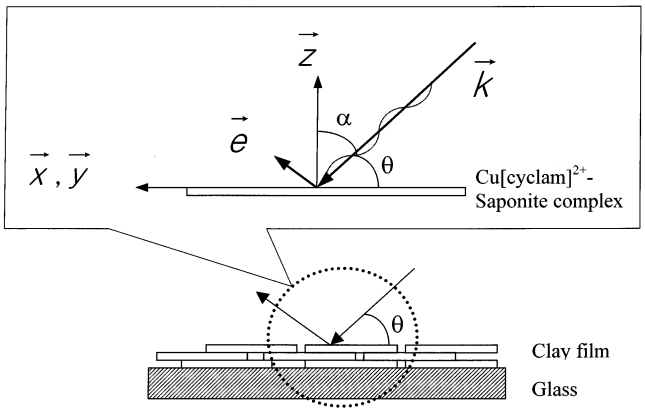

Figure 4. Schematic description of the polarized XAS experiment, where k is the X-ray propagation direction, $\vec{e}$ is the polarization direction, (x, y), which is parallel to the Cu−N_4 plane, z is perpendicular to the Cu−N_4 plane, and θ represents the angle between k and the z axis.

Polarized Cu K-Edge XANES Spectra. Because the XANES spectra for powdered samples are superposed in all edge transitions for both the bound state and the continuum regimes, all the peak have been assigned indistinctly, moreover, often incorrectly. To solve this problem, we conducted polarization-dependent XAS measurements for the oriented $[Cu(cyclam)]^{2+}$−saponite film at several angles between two configurations parallel ($\vec{e}\|c$) and perpendicular ($\vec{e}\perp c$) to the c axis, where $\vec{e}$ denotes the X-ray polarization vector. However, the orientation effect must be carefully checked to acquire some knowledge from peak intensities in XANES spectra for layered materials because there are severe intensity variations depending on the angles.

The complex used in this study is the square-planar Cu(II) with a single-ligand coordination center, CuN_4, where N refers to the ligation through the nitrogen atoms of the heterocyclic planar ligands. The molecular axis system is defined by having the z axis perpendicular to the average CuN_4, which is nearly coincident with the axes of layered aluminosilicate because the CuN_4 plane runs parallel to the basal plane of saponite sheets. The x and y axes are defined as two orthogonal axes in this plane lying approximately along the Cu−N bonds. The polarized spectra are described by the orientation of the polarization direction ($\vec{e}$) with respect to the molecular axis z. A schematic summary of the molecular orientation is presented in Figure 4.

Figure 5 shows the angle-dependent XANES spectra and their second derivatives for the $[Cu(cyclam)]^{2+}$−saponite film. The first peak (A) around 8979 eV reveals the preedge due to the 1s → 3d transition, which is predominant in the absence of inversion symmetry.[22] However, no intensity variation of the preedge with respect to the incident angle was observed, implying that the local symmetry of the $[Cu(cyclam)]^{2+}$ ion with inversion symmetry remains unchanged in the interlayer space of saponite.[23]

It is worthwhile to note here that the second peak (B) at 8984.5 eV shows a strong intensity variation depending upon the incident angle without any shift of peak position. This peak can be definitely assigned to the 1s → ($4p_z$ + L) shake-down transition involving a 1s → $4p_z$ transition with simultaneous ligand-to-metal charge transfer (LMCT) by means of the Cu K-edge XANES studies.[24−28] That is, the core hole of the final state is stabilized by additional screening due to electron transfer from the ligand p orbital to the metal d orbital so that the dipolar transition can occur at a lower energy compared to that of the

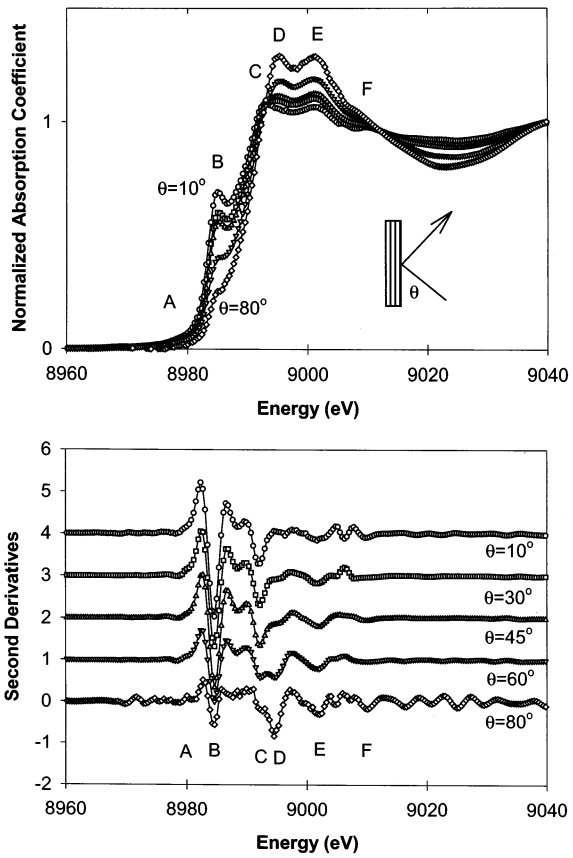

Figure 5. Angle-resolved Cu K-edge XANES spectra and their second derivatives for the [Cu(cyclam)]$^{2+}$−saponite film.

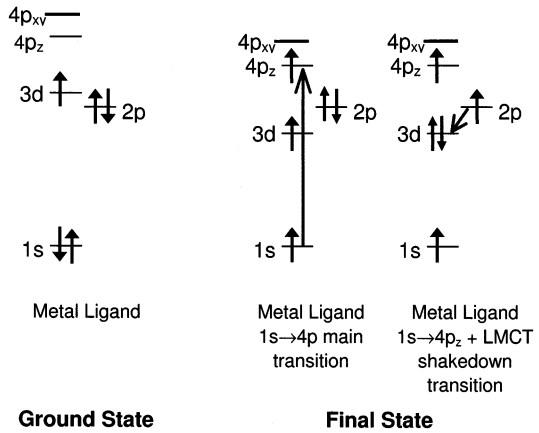

Figure 6. Schematic description of the ligand-to-metal charge-transfer (LMCT) transition.

nonadditional screening effect due to the charge transfer (Figure 6). Because this transition is due to the *z* component, the intensity increases gradually from 80 to 10° with respect to the incident X-ray beam, as shown in Figure 5.

In the next main edge region around 8990 eV due to the transition of 1s → 4p, peak C at 8992 eV becomes dominant, and peak D at 8995.2 eV decreases as the incident angle decreases, as shown in Figure. 5. Therefore, we can assign the former to the 1s → 4p$_z$ transition ($\vec{e}\|z$) and the latter to the 1s → 4p$_{xy}$ transition ($\vec{e}\perp z$),[28] which is different from the previous assignment, where these peaks could not be distinguished in nonpolarized XANES data from those in the powder sample.[10,11] However, peaks E around 9002 and 9009 eV are slightly enhanced, depending on the incident angle, which can be explained by multiple scattering (MS) effects that are mainly

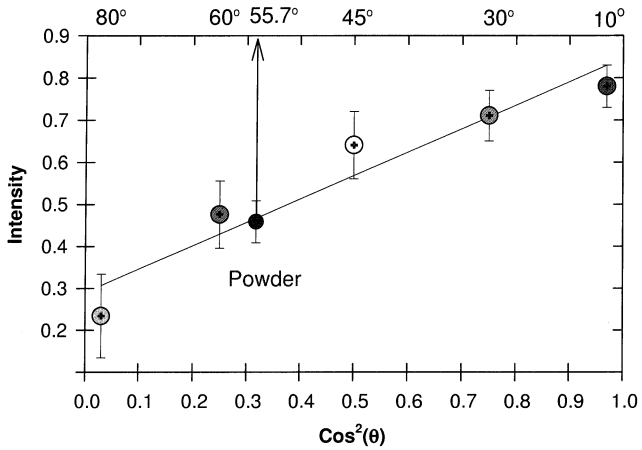

Figure 7. Relation between the intensity of the peak due to LMCT and the incident angles in the Cu K-edge XANES spectra for the [Cu(cyclam)]$^{2+}$−saponite film. It should be noted that the powder value is consistent with 55.3° (magic angle) interpolated from the intensity of the film.

due to the in-plane component at the continuum state or by the penetration of EXAFS.[29]

For the lamella compounds with a symmetry axis higher than that of the 2-fold axis perpendicular to the plane, the absorption coefficient, μ, is independent of the polarization in the layered planes (*x*- and *y*-axis components) but is dependent on the out-of-plane (*z*-axis) component, as in the following relation:[30]

$$\mu(\alpha) = (\mu_{\|} - \mu_{\perp}) \cos^2 \alpha + \mu_{\perp}$$

where α is the angle between the polarization vector ($\vec{e}$) and the layer plane that is equal to ($90° - \theta$) with respect to the incident angle θ. This relation applies at each energy and can be used to determine, via a linear regression and an extrapolation, the coefficient $\mu_{\perp}$, which cannot be measured experimentally ($\alpha = 90°$). Because the sample thickness that is penetrated by the X-ray beam increases with α, the absorption value measured at each energy must be multiplied by $\cos(\alpha)$ before on can calculate $\mu_{\perp}$.[29]

In Figure 7, we plot the observed peak intensity of the 1s → 4p$_z$ + shakedown transition versus $\cos^2 \theta$. Ideally, such a plot would be a straight line through the origin if the dipole interaction contributes only to the peak intensity, but an incomplete polarization in the incident X-ray beam and disorder of [Cu(cyclam)]$^{2+}$ ion in the interlayer space may give rise to a slight contribution in the background intensity in the zero $\vec{e}$ component. It should be noted that the intensity for the powder sample is located at $\theta \approx 50°$, which is nearly identical to the magic angle, 55.7°, where $\mu_{\text{powder}} = (^2/_3\mu_{\|}) + (^1/_3\mu_{\perp})$. Therefore, it is thought that the orientation effect is insignificant in the present powder sample, which may be due to either the poor crystallinity and small crystal size of the present host, saponite, or to the incomplete ordering of guest molecules in the interlayer space.

In the above XANES and XRD results, showing that the plane of the [Cu(cyclam)]$^{2+}$ ion in the interlayer space parallels the clay sheets, we were able to determine the origin of each peak successfully. It should be also noted here that it is possible to predict reversibly the orientation of guest species in an intercalation complex by using a polarized XANES experiment if we have some polarized XANES information for the single crystal of the guest molecule.

XANES Spectra for Powder Samples. Figure 8 and Table 1 represent the Cu K-edge XANES spectra and their second

TABLE 1: Peak Positions (eV) and Assignments for XANES Spectra for the [Cu(cyclam)]$^{2+}$−Saponite Complex and for [Cu(cyclam)](ClO$_4$)$_2$ and Its Aqueous Solution[a]

compounds	A (1s → 3d)	B (1s → 4p$_z$ + shakedown)	C (1s → 4p$_z$)	D (1s → 4p$_{xy}$)	E (MS)[d]
[Cu(cyclam)](ClO$_4$)$_2$	8978.8	8985.8	8993.1	8994.9	9001.1
[Cu(cyclam)]$^{2+}$ solution	8978.8	8985.7(−0.1)	8993.1(0.0)	8995.1(+0.4)	9000.9(+0.2)
[Cu(cyclam)]$^{2+}$−saponite	8978.8	8984.7(−1.1)	8992.1(−1.0)	8995.1(+0.2)	9001.7(+0.6)
[Cu(cyclam)]$^{2+}$−montmorillonite[b]	8978.8	8984.1(−1.7)	8992.1(−1.0)	8995.0(+0.1)	9001.5(+0.4)
[Cu(cyclam)]$^{2+}$−hectorite[c]	8978.8	8984.4(−1.4)	8992.2(−0.9)	8995.1(+0.2)	9001.7(+0.6)

[a] Error in energy is ±0.1 eV, and the values in parentheses represent the difference from the energy for [Cu(cyclam)](ClO$_4$)$_2$. [b] From ref 10. [c] From ref 11. [d] Multiple scattering.

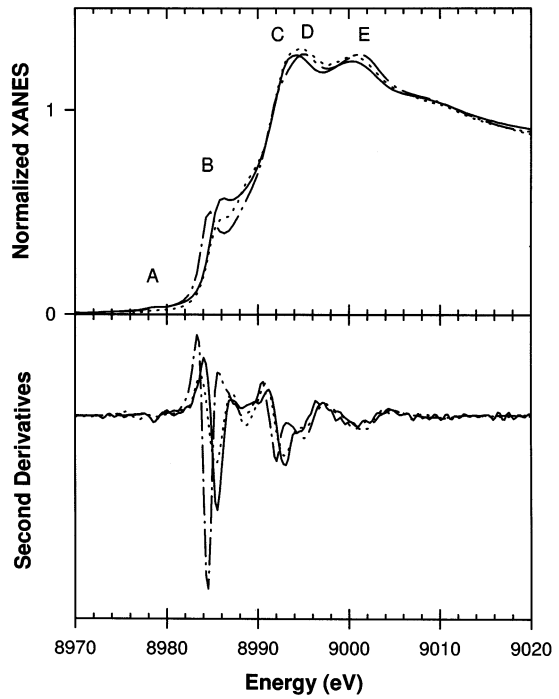

Figure 8. Cu K-edge XANES spectra and their second derivatives for [Cu(cyclam)]$^{2+}$−saponite (− · −) and for [Cu(cyclam)](ClO$_4$)$_2$ (—) and its aqueous solution (· · ·).

derivatives for [Cu(cyclam)]$^{2+}$−saponite and for [Cu(cyclam)](ClO$_4$)$_2$ and its aqueous solution. Peak A due to the 1s → 3d transition was nearly unchanged upon intercalation, demonstrating that the valence state of divalent copper and its square-planar symmetry remain unaffected. However, peak B due to the 1s → 4p$_z$ + shakedown transition in the intercalate shifts to lower energy by approximately 1.1 eV compared to that for [Cu(cyclam)](ClO$_4$)$_2$. This energy shift reflects an enhanced bond covalency between copper and nitrogen ligands.[10,11] Previously, we suggested that the energy of this shakedown transition is strongly related to the (Cu—N) bond covalency, induced by the charge transfer from the 2p orbitals of the nitrogen ligand to the 3d orbitals of the copper metal.[10] However, because this peak is highly influenced by the orientation of the [Cu(cyclam)]$^{2+}$ ion, as indicated above in the angle-dependent experiment, the transition is also related to the (Cu—O$_{axial}$) bond distance. In montmorillonite and hectorite intercalated with [Cu(cyclam)]$^{2+}$ ions, the energy shifts of this peak were estimated to be 1.7 and 1.4 eV, respectively, whereas their basal increment was 3.86 and 3.81 Å.[10,11] Even though the axial oxygen was not observed in the EXAFS spectra of [Cu(cyclam)]$^{2+}$-intercalated montmorillonite and hectorite, the [Cu(cyclam)]$^{2+}$ ion may experience a negative layer charge in the octahedral sheet of the montmorillonite or hectorite lattice at a greater distance compared to that of [Cu(cyclam)](ClO$_4$)$_2$. The present [Cu(cyclam)]$^{2+}$−saponite complex shows a basal increment of 3.72 Å, which is slightly shorter than that of montmorillonite intercalate.

Owing to a smaller basal increment as well as the shorter distance of the negative layer charge in the tetrahedral sheet, the [Cu(cyclam)]$^{2+}$ ion can experience the negative charge at a shorter distance compared to the montmorillonite complex. Such a short distance from the negative point charge makes the d_{z^2} orbital of Cu metal unstable, which thereby induces the stabilization of the half-filled $d_{x^2-y^2}$ antibonding orbital. This causes the LMCT to become ineffective, and the covalent character of the (Cu—N) bond along the equatorial plane becomes weaker than that for the case of the montmorillonite complex. Such a situation is also confirmed by the peak intensity in the XANES spectrum for [Cu(cyclam)](ClO$_4$)$_2$, where the bond distance between copper and oxygen is very short (i.e., 2.567 Å), showing that it is within an ionocovalent bonding region. The very short distance between copper and axial oxygen gives rise to more ineffective LMCT between copper and equatorial nitrogen ligands, resulting in a weak transition probability compared to that for the intercalation complex, as shown in Figure 8 (bottom).

Such a difference in covalency between copper and nitrogen shifts the peak to a lower energy in the intercalation complexes compared to the peak position in [Cu(cyclam)](ClO$_4$)$_2$. Therefore, it was confirmed that the amount of (Cu—N) bond covalency increases in the following sequence: [Cu(cyclam)]$^{2+}$−montmorillonite > [Cu(cyclam)]$^{2+}$−hectorite > [Cu(cyclam)]$^{2+}$−saponite ≫ [Cu(cyclam)](ClO$_4$)$_2$.

The increased covalency between copper and equatorial nitrogen ligands compared to [Cu(cyclam)](ClO$_4$)$_2$ induces the stabilization of the out-of-plane component and the destabilization of the in-plane component. Because these transitions correspond to those from the 1s to the antibonding 4p orbitals, the energy position of peak C due to the 1s → 4p$_z$ transition is consistent with such a scheme in the XANES spectrum for the [Cu(cyclam)]$^{2+}$−saponite complex, where peak C shows a lower energy shift of ca. 1.0 eV compared to that of [Cu(cyclam)](ClO$_4$)$_2$. However, the energy position of peak D due to the 1s → 4p$_{xy}$ transition shifts slightly to a higher energy by ca. 0.2 eV.

The other peak at around 9002 eV due to either the MS effects or the penetration of EXAFS at the continuum state shows a higher energy shift of ca. 0.9 eV. Previously, Bianconi et al. proved that this MS peak position is highly related to the bond distance between the central atom and the first nearest neighbors.[31] The bond distance becomes short as the energy shift increases. Therefore, the above energy shift of the MS peak in the [Cu(cyclam)]$^{2+}$−saponite complex reflects the shortening of the (Cu—N) bond due to the increment of the bond covalency.

EXAFS Spectra for Powder Samples. Figure 9 shows the k^3-weighted EXAFS oscillations and their Fourier transforms (FTs) in the range ∼2.3 Å^{-1} < k < 14.3 Å^{-1}. The first peak

TABLE 2: EXAFS Fitting Results for $[Cu(cyclam)](ClO_4)_2$ and $[Cu(cyclam)]^{2+}$−Saponite[a]

compounds	atom pair	CN[b]	R (Å)[b]	E_0 (eV)[b]	σ^2 ($\times 10^{-3}$ Å^2)[b]	R factor
$[Cu(cyclam)](ClO_4)_2$	Cu—N	4	2.02	0.54	4.30	0.008
	Cu—O	2	2.54		14.6	
	Cu- - -C	4	2.82		1.71	
	Cu- - -C	4	3.00		1.94	
	Cu- - -C	2	3.42		3.28	
$[Cu(cyclam)]^{2+}$−saponite	Cu—N	4	2.01	2.24	3.92	0.001
	Cu- - -C	4	2.84		4.58	
	Cu- - -C	4	3.01		3.64	
	Cu- - -C	4	3.43		2.16	
	Cu—O	2	3.80		29.7	

[a] Fitting range for k is 3.5−12.5 Å^{-1}, and for R, is 0.50−3.85 Å. The number of independent points is 14, and that of fitting variables is 12. [b] Errors for CN (coordination number) and σ^2 (Debye−Waller factor) are 20%, and for R (interatomic distance) and E_0 (threshold energy difference), they are 0.02 Å and 1.8 eV, respectively.

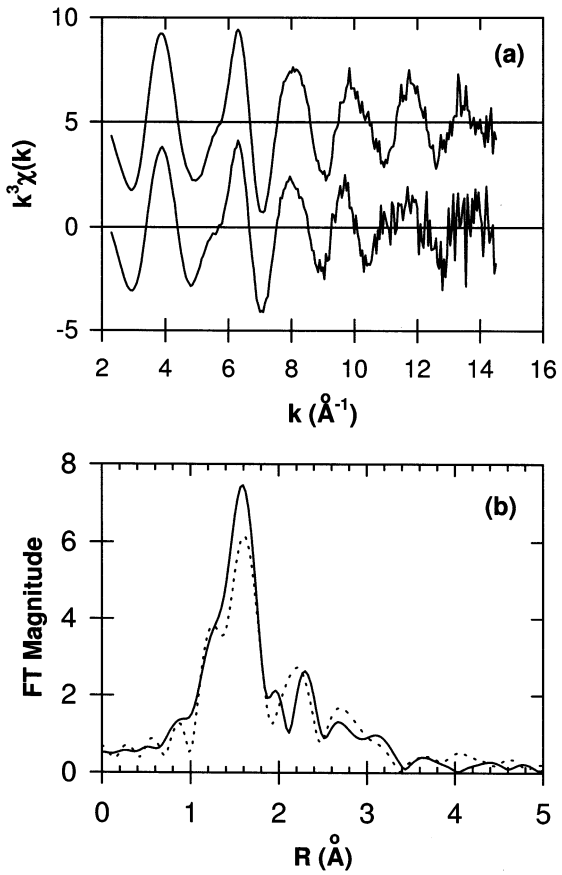

Figure 9. Cu K-edge EXAFS spectra (top) and their Fourier transforms (bottom) for the $[Cu(cyclam)]^{2+}$−saponite powder (—) and $[Cu(cyclam)](ClO_4)_2$ (• • •).

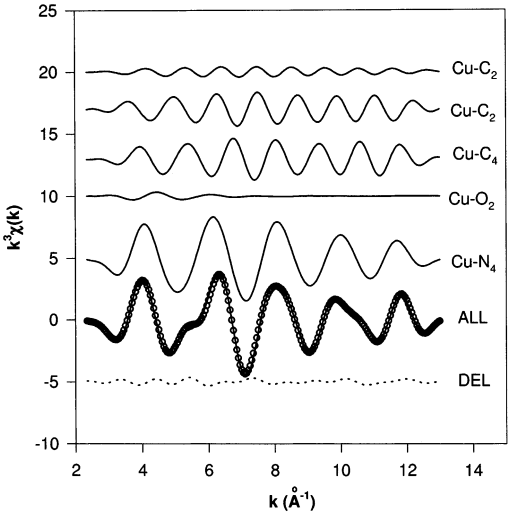

Figure 10. EXAFS fitting result for $[Cu(cyclam)](ClO_4)_2$ including experimental (○) and fitting results (—). DEL represents the deviation between the experimental results and the fit.

around 1.6 Å is due to the first nitrogen ligand, and the additional peaks up to ~3.3 Å correspond to the outer Cu—O and Cu- - -C shells. Another interesting feature in the FTs is that the intercalated copper complex shows a larger intensity in the first peak than that for the $[Cu(cyclam)](ClO_4)_2$ salt.

For the quantitative analysis of the structural data, nonlinear least-squares curve fitting has been carried out. For the $[Cu(cyclam)](ClO_4)_2$ salt, the multishell fittings have been performed in the range 0.5 Å < R < 3.5 Å to obtain the local structural parameters because contributions of the axial (Cu—O) bonds and the nonbonded Cu- - -C interactions, as well as the equatorial (Cu—N) bonds, to EXAFS oscillation significantly interfere with one another so that each contribution to the EXAFS oscillation could not be well resolved. The best-fit structural parameters are presented in Table 2, and the inverse FTs, $k^3\chi(k)$, of the fitted regions on FTs are compared with theoretical spectra depicted by using the obtained parameters (Figure 10). The best-fit distances are shown to be in good agreement with the crystallographically determined distances within the experimental error limit (± 0.02 Å).[19]

EXAFS spectra for the intercalated copper complex were analyzed in the same manner as for its salt compound (Figure 11). From these EXAFS analyses, it is clearly understood that the average Cu- --C distances for the salt compound are hardly changed by the intercalation. However, it should be noted that the bond distance of (Cu—N) is shorter and that of (Cu—O) is longer than those for the $[Cu(cyclam)](ClO_4)_2$ salt. The Debye−Waller factor, which reflects the static/dynamic disorder, of the (Cu—N) bond in the intercalation complex is significantly decreased, implying that the bond covalency between copper and nitrogen becomes stronger than that of the free salt compound. This result is consistent with the above-mentioned XANES results.

We emphasize that, in the $[Cu(cyclam)]^{2+}$−saponite complex, the six oxygen ligands are observed at a long distance of about 3.8 Å, which is different from that of the $[Cu(cyclam)]^{2+}$−montmorillonite complex.[10] Because the gallery height of 3.7 Å indicates that only a monolayer of $[Cu(cyclam)]^{2+}$ ions is stabilized in the interlayer space of the host lattice, this distant (Cu−O) shell must originate from the silicate lattice of saponite. However, the value is greater than the sum (2.9 Å) of the van der Waals radii of 1.5 Å for the oxygen atom and 1.4 Å for the Cu atom; therefore, there is no bonding character between copper and oxygen,[32] which is consistent with the large Debye−Waller factor.[33]

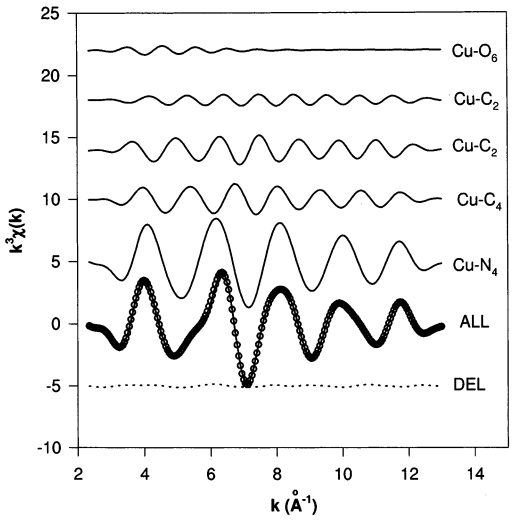

Figure 11. EXAFS fitting result for the $[Cu(cyclam)]^{2+}$−saponite powder including experimental (○) and fitting results (−). DEL represents the deviation between the experimental results and the fit.

Considering the in-plane structure of the host silicate sheet in saponite, we find that two possible sites are available for the intercalated cation, as previously indicated in the montmorillonite complex.[10] One site is located between the triangular basal oxygen atoms of the SiO_4 tetrahedra, and the other is the ditrigonal cavity often described as the siloxane ring. Oxygen ligands serve as probes for the $[Cu(cyclam)]^{2+}$ ion to be located at the former site among the available positions, which are different from those of the saponite complex. Because the negative charge originates from isomorphous substitution in the tetrahedral site from Si^{4+} to Al^{3+}, in the case of saponite, it is possible for the copper complex to be located at such a position.

Conclusions

In the present study, we have successfully assigned all the peaks in the Cu K-edge XANES spectra by performing a polarization XAS experiment for oriented $[Cu(cyclam)]^{2+}$−saponite films as in-plane components and out-of plane components. On the basis of the peak assignments from the polarization experiment, it is possible to assign each peak in the XANES spectra of powdered samples; these peaks are ambiguous in the previous unpolarized experiment because of the serious overlap of each component. The dominant change in the $1s \rightarrow 4p_z + L$ (LMCT) peak was observed in the XANES spectra of the powdered samples after the ion-exchange reaction; this change is due to the change in covalent character between the central copper and equatorial nitrogen ligands of $[Cu(cyclam)]^{2+}$ complexes. The covalency of the Cu−N bond increases in the following order: $[Cu(cyclam)]^{2+}$−montmorillonite > $[Cu(cyclam)]^{2+}$−hectorite > $[Cu(cyclam)]^{2+}$−saponite ≫ $[Cu(cyclam)](ClO_4)_2$, which is consistent with the stabilized out-of-plane and destabilized in-plane components. The bond distance between Cu and nitrogen becomes shorter, but the bond distance between Cu and the axial ligand, oxygen, becomes longer after the intercalation. The structural change is well explained by the amount of layer charge and the origin of the charge deficiency of aluminosilicates.

From the present experimental findings, it becomes clear that XAS is a powerful tool for determining the orientation and location of the intercalated guest molecules in the interlayer space of layered materials and for analyzing the host−guest interaction in this intercalation complex. The location and orientation of guest ions within the interlayer space in layered aluminosilicate can be strongly influenced by the magnitude of layer charge and its source and by the clay type, trioctahedral or dioctahedral. This has led us to conduct a systematic study of host−guest interactions with respect to the electronic and structural influences of the host matrix on guest molecules by employing various types of clays.

Acknowledgment. This study was supported by the National Research Laboratory program (NRL 1999). We thank Professor M. Nomura for his help in synchrotron radiation experiments conducted at the Photon Factory.

References and Notes

(1) *Intercalation Chemistry*; Whittingham, M. S., Jacobson, A. J., Eds.; Academic Press: New York, 1982.
(2) Pinnaviaia, T. J. *Science (Washington, D.C.)* **1983**, *220*, 365.
(3) *Pillared Clays*; Bruch, R., Ed.; Catalysis Today; Elsevier: Amsterdam, 1988; Vol. 2.
(4) Choy, J.-H.; Park, J.-H.; Yoon, J.-B. *J. Phys. Chem. B* **1998**, *102*, 5991.
(5) Choy, J.-H.; Yoon, J.-B.; Kim, D.-K.; Hwang, S.-H. *Inorg. Chem.* **1995**, *35*, 3513.
(6) Choy, J.-H.; Kim, D.-K.; Hwang, S.-H.; Demazeau, G.; Jung, D.-Y. *J. Am. Chem. Soc.* **1995**, *117*, 8557.
(7) Michalowicz, A.; Verdaguer, M.; Mathey, Y.; Clement, R. In *Synchrotron Radiation in Chemistry and Biology;* Mandelkow, E., Ed.; Topics in Current Chemistry; Springer-Verlag: Berlin, 1988; Vol. 1, pp 107−149.
(8) Abb, F.; Santis, G. D.; Fabbrizzi, L.; Licchelli, M.; Lanfredi, A. M.; Pallavicini, P.; Poggi, A.; Ugozzoli, F. *Inorg. Chem.* **1994**, *33*, 1366.
(9) Martire, D. O.; Jux, N.; Aramendia, P. F.; Negri, R. M.; Lex, J.; Braslavsky, S. E.; Schaffner, K.; Vogel, E. *J. Am. Chem. Soc.* **1992**, *114*, 9969.
(10) Choy, J.-H.; Kim, D.-K.; Park J.-C.; Choi S.-N.; Kim, Y.-J. *Inorg. Chem.* **1997**, *36*, 189.
(11) Choy, J.-H.; Kim, B.-W.; Park, J.-C.; Yoon, J.-B. *Mol. Cryst. Liq. Cryst.* **1998**, *311*, 303.
(12) Ebina, T.; Iwasaki, T.; Chatterjee, A.; Katagiri, M.; Stucky, G. D. *J. Phys. Chem. B* **1997**, *101*, 1125.
(13) Teo, B. K. *EXAFS: Basic Principles and Data Analysis*; Springer-Verlag: Berlin, 1986; pp 114−157.
(14) Sayers, D. E.; Bunker, B. A. In *X-ray Absorption: Principles, Applications, Techniques of EXAFS, SEXAFS, and XANES*; Konigsberger, D. C., Prins, R., Eds.; Wiley-Interscience: New York, 1989; pp 211−253.
(15) Lytle, F. W. In *Applications of Synchrotron Radiation*; Winick, H., Xian, D., Ye, M., Huang, T., Eds.; Gordon and Breach Science: New York, 1989; pp 135−223.
(16) Stern, E. A.; Newville, M.; Ravel, B.; Yacoby, Y.; Haskel, D. *Physica B* **1995**, *208/209*, 117.
(17) Rehr, J. J. *Jpn. J. Appl. Phys.* **1993**, *32*, 8.
(18) Rehr, J. J.; Zabinsky, S. I.; Albers, R. C. *Phys. Rev. Lett.* **1992**, *69*, 3397.
(19) Tasker, P. A.; Sklar, L. *J. Cryst. Mol. Struct.* **1975**, *5*, 329.
(20) Grim, R. E. *Clay Mineralogy*; McGraw-Hill International Series in the Earth and Planetary Sciences; McGraw-Hill: New York, 1968.
(21) Carrado, K. A.; Wasserman, S. R. *Chem. Mater.* **1996**, *8*, 219−225.
(22) Sano, M.; Komorita, S.; Yamatera, H. *Inorg. Chem.* **1992**, *31*, 459.
(23) Hahn, J. E.; Scott, R. A.; Hodgson, K. O.; Doniach, S.; Desjardins, S. R.; Solomon, E. I. *Chem. Phys. Lett.* **1982**, *88*, 595.
(24) Choy, J.-H.; Kim, D.-K.; Hwang, S.-H.; Demazeau, G. *Phys. Rev. B* **1994**, *50*, 16631.
(25) Shadle, S. E.; Penner-Hahn, J. E.; Schugar, H. J.; Hedman, B.; Hodgson, K. O.; Solomon, E. I. *J. Am. Chem. Soc.* **1993**, *115*, 767.
(26) Kau, L.-S.; Spira-Solomon, D. J.; Penner-Hahn, J. E.; Hodgson, K. O. *J. Am. Chem. Soc.* **1987**, *109*, 6433.
(27) Yokoyama, T.; Kosugi, N.; Kuroda, H. *Chem. Phys.* **1986**, *103*, 101.
(28) Kosugi, N.; Yokoyama, T.; Asakura, K.; Kuroda, H. *Chem. Phys.* **1984**, *91*, 249.
(29) Waychunas, G. A.; Brown, G. E., Jr. *Phys. Chem. Miner.* **1990**, *17*, 420.
(30) Heald, S. M.; Stern, E. A. *Phys. Rev. B* **1977**, *16*, 5549.
(31) Garcia, J.; Benfatto, M.; Natoli, C. R.; Bianconi, A.; Fontaine, A.; Tolentino, H. *Chem. Phys.* **1989**, *132*, 295.
(32) Huheey, J. E.; Keiter, E. A.; Keiter, R. L. *Inorganic Chemistry: Principles of Structure and Reactivity*, 4th ed.; Harper Collins: New York, 1993; p 292.
(33) Sayers, D. E.; Stern, E. A.; Lytle, F. W. *Phys. Rev. Lett.* **1971**, *27*, 1204.